Available online at www.sciencedirect.com
ScienceDirect
Journal of Bionic Engineering 5 (2008) 159−165

Research on the Swing of the Body of Two-Joint Robot Fish

Ying-xiang Liu, Wei-shan Chen, Jun-kao Liu

School of Mechatronics Engineering, *Harbin Institute of Technology*, *Harbin* 150001, *P. R. China*

Abstract

The disadvantages caused by the swing of a fish body were analyzed. The coordinate system of a two-joint robot fish was built. The hydrodynamic analysis of robot fish was developed. The dynamic simulation of a two-joint robot fish was carried out with the ADAMS software. The relationship between the swing of fish body and the mass distribution of robot fish, the relationship between the swing of fish body and the swing frequency of tail, were gained. The impact of the swing of fish body on the kinematic parameters of tail fin was analyzed. Three methods to restrain the swing of fish body were presented and discussed.

Keywords: robot fish, swing of fish body, hydrodynamic analysis, dynamic simulation

1 Introduction

The robot fish is a focus in bionic research, and the dynamics of robot fish has not been fully understood yet. Wu[1] presented the "Two-dimensional Waving Plate Theory" to analyze the dynamics of *Carangiform* fish in 1961. Lightill[2] utilized the "Elongated-body Theory" to study the dynamics of *Carangiform* fish in 1970. Considering the change of the heaving amplitude of tail fin, Lightill[3] presented the "Large Amplitude Elongated-body Theory" in 1971. In 1977, Chopra and Kambe[4] developed the "Two-dimensional Resisting Force Theory" adapted to the large amplitude propulsive system with lunate tail fin. Tong *et al*.[5] presented the "Three-dimensional Waving Plate Theory" to analyze the accelerated performance of fish and the evolution of trailing vortex. Su *et al*.[6] studied the hydrodynamic force of tail fin by dividing the surface of tail fin to minute elements.

People have done vast research on the dynamics of fish, but few attentions were paid to the swing of fish body in the dynamic analysis of robot fish. The swing of fish body could make the heaving motion amplitude and the attack angle of tail fin deviate from the optimal values, and hence reduce the propulsive force and efficiency. Furthermore, the swing of fish body would damage the propulsive stability, impact the reliable operating of sensor-based system.

We present our study in the following four sections. The coordinate system of two-joint robot fish is built in Section **2**. In Section **3**, the hydrodynamic analysis of two-joint robot fish is developed. In Section **4**, the dynamic simulation of a two-joint robot fish was conducted with the ADAMS software to study the swing of fish body, and three methods to restrain the swing of fish body are presented and discussed. The conclusion is summarized in Section **5**.

2 Foundation of coordinate system

As the two-joint robot fish is the most fundamental type, we take it to proceed the research. Fig. 1 shows the basic structure of two-joint robot fish, which contains a fish body, a tail and a tail fin. There is a rotational joint between the fish body and tail, and another rotational joint between the tail and tail fin. The robot fish gains propulsive force by pitching motion of the tail and tail fin.

Fig. 2 shows the coordinate system of two-joint robot fish. The origin points, O_1, O_2 and O_3, are on the center line of robot fish. The origin point O_1 is the

Corresponding author: Ying-xiang Liu
E-mail: liuyingxiang868@163.com

barycenter of fish body. O_2Z_2 is the axial line of the rotational joint between the fish body and tail. O_3Z_3 is the axial line of the rotational joint between the tail and tail fin. $O-XYZ$ is the static coordinate system. $O_1-X_1Y_1Z_1$ is the dynamic coordinate system of fish body. $O_2-X_2Y_2Z_2$ is the dynamic coordinate system of tail. $O_3-X_3Y_3Z_3$ is the dynamic coordinate system of tail fin.

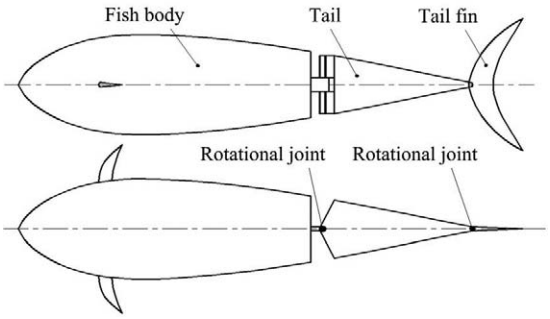

Fig. 1 Structure of the two-joint robot fish.

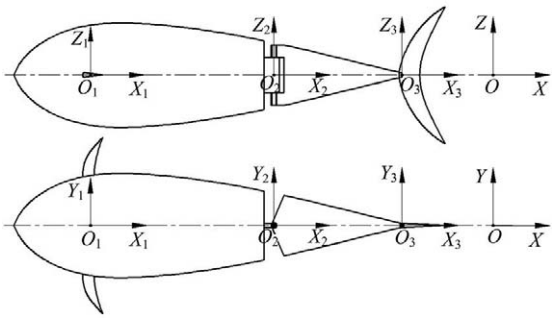

Fig. 2 Coordinate system of the two-joint robot fish.

The attack angle of tail fin is the angle between the center line of tail fin and the tangent of the trace of point O_3. The heaving motion amplitude of tail fin is the projection of the distance between two adjacent extreme positions of point O_3 on the direction normal to the swimming orientation of robot fish. The swing amplitude of fish body is the sum of the angles between two adjacent extreme positions of the center line of fish body and the swimming orientation of robot fish.

3 Hydrodynamic analysis of robot fish

3.1 Force analysis of robot fish

The swimming principle of fish is very complicated. The domain of the Reynolds number, Re, during the swimming of *Thunniform* fish is 10^5-10^8, and in this domain the viscous force could be ignored because it is very small compared with the apparent force[7].

Fig. 3 shows the force analysis of robot fish on the condition that the underwater depth of robot fish keeps unchanged. The tail and tail fin are simplified to flat plates with large rigidity. The hydrodynamic forces of fish body are divided to a equivalent force $\boldsymbol{F}_{1X}$ along OX, a equivalent force $\boldsymbol{F}_{1Y}$ along OY and a equivalent resistance moment $\boldsymbol{M}_1$ around O_1Z_1. $\boldsymbol{F}_2$ is the equivalent force of the tail. L_6 is the distance between O_2 and the action spot of $\boldsymbol{F}_2$. $\boldsymbol{F}_3$ is the equivalent force of the tail fin. L_7 is the distance between O_3 and the action spot of $\boldsymbol{F}_3$. $\boldsymbol{M}_2$ is the driving moment of the rotational joint between fish body and tail. $\boldsymbol{M}_3$ is the driving moment of the rotational joint between tail and tail fin. Nearly 90% propulsive force of *Thunniform* fish is from the tail fin[7], so in the following study set the hydrodynamic force of tail as $\boldsymbol{F}_2 = 0$.

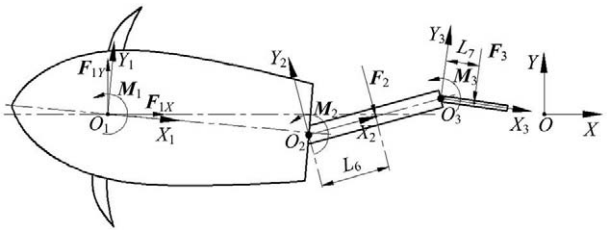

Fig. 3 Force analysis of the two-joint robot fish.

3.2 Hydrodynamic model of fish body

In irrotational, inviscid and incompressible fluid, utilizing the Bernoulli equation, the pressure on the surface of a body is given as[6]:

$$p_1(t) = p_0 + \frac{1}{2}\rho[|V_0(t)|^2 - |V_1(t)|^2] - \rho\frac{\partial\phi(t)}{\partial t}, \qquad (1)$$

where $V_0(x,y,x,t)$ is the current velocity of the fluid, $p_1(t)$ is the pressure of point $P_1(x,y,z,t)$ on the surface of the body, p_0 is the pressure of point $Q(x_0,y_0,z_0)$ on the border, ρ is the density of fluid, $V_1(t)$ is the resultant velocity of point P_1, $\phi(t)$ is the disturbed velocity potential of point P_1.

The pressure function $p_1(x,y,z,t)$ on the surface of fish body could be developed from Eq. (1). Dividing the surface of fish body to minute elements, dS indicates a random surface element, (x,y,z) is the position of the center of dS in the coordinate system $O-XYZ$,

(x_1, y_1, z_1) is the position of the center of $\mathrm{d}S$ in the coordinate system $O_1 - X_1Y_1Z_1$, then the force on element $\mathrm{d}S$ is given as:

$$\mathrm{d}\boldsymbol{F} = [-p_1(x, y, z, t)\mathrm{d}S]\boldsymbol{n}_S, \tag{2}$$

where $\boldsymbol{n}_S$ is the unit normal vector of $\mathrm{d}S$.

The component of $\mathrm{d}\boldsymbol{F}$ on OX is given by the relationship:

$$\mathrm{d}\boldsymbol{F}_X = \mathrm{d}\boldsymbol{F} \bullet \boldsymbol{n}_X = [-p_1(x, y, z, t)\mathrm{d}S]\boldsymbol{n}_S \bullet \boldsymbol{n}_X. \tag{3}$$

The component of $\mathrm{d}\boldsymbol{F}$ on OY is given by the relationship:

$$\mathrm{d}\boldsymbol{F}_Y = \mathrm{d}\boldsymbol{F} \bullet \boldsymbol{n}_Y = [-p_1(x, y, z, t)\mathrm{d}S]\boldsymbol{n}_S \bullet \boldsymbol{n}_Y. \tag{4}$$

Then $\boldsymbol{F}_{1X}$, $\boldsymbol{F}_{1Y}$ and $\boldsymbol{M}_1$ could be given by the relationships:

$$\boldsymbol{F}_{1X} = \iint_{S_B} \mathrm{d}\boldsymbol{F}_X = \iint_{S_B} [-p_1(x, y, z, t)]\boldsymbol{n}_S \bullet \boldsymbol{n}_X \mathrm{d}S, \tag{5}$$

$$\boldsymbol{F}_{1Y} = \iint_{S_B} \mathrm{d}\boldsymbol{F}_Y = \iint_{S_B} [-p_1(x, y, z, t)]\boldsymbol{n}_S \bullet \boldsymbol{n}_Y \mathrm{d}S, \tag{6}$$

$$\begin{aligned} \boldsymbol{M}_1 &= \iint_{S_B} \left(\mathrm{d}\boldsymbol{F}_Y x_1 - \mathrm{d}\boldsymbol{F}_X y_1\right) \\ &= \iint_{S_B} [p_1(x, y, z, t)]\boldsymbol{n}_S \bullet (\boldsymbol{n}_X y_1 - \boldsymbol{n}_Y x_1)\mathrm{d}S, \end{aligned} \tag{7}$$

where S_B is the exterior surface of fish body.

Define C_{1X} indicates the drag coefficient of propulsion, C_{1Y} indicates the drag coefficient of side movement, C_{1S} indicates the drag coefficient of the swing of fish body. C_{1X}, C_{1Y} and C_{1S} are given by Eq. (8). The exact value of C_{1X}, C_{1Y} and C_{1S} could be gained by underwater test.

$$\begin{cases} C_{1X} = \dfrac{F_{BX}}{\rho V_{XO_1}^2 A_X / 2} \\ C_{1Y} = \dfrac{F_{BY}}{\rho V_{YO_1}^2 A_Y / 2} \\ C_{1S} = \dfrac{M_1}{\rho \dot{\theta}_{10}^2 [(L_0 - L_1)^4 / L_1 + L_1^3] A_Y / 8} \end{cases}, \tag{8}$$

where F_{BX} is the component of the hydrodynamic force of fish body on O_1X_1, V_{XO_1} is the component of the velocity of O_1 on O_1X_1, A_X is the projection area of fish body on the plane $Y_1O_1Z_1$, F_{BY} is the component of the hydrodynamic force of fish body on O_1Y_1, V_{YO_1} is the component of the velocity of O_1 on O_1Y_1, A_Y is the projection area of fish body on the plane $X_1O_1Z_1$, θ_{10} is the angle between O_1X_1 and OX, L_0 is the length of fish body, L_1 is the distance between O_1 and O_2.

The transformation between F_{BX}, F_{BY}, F_{1X} and F_{1Y} is given by the relationships:

$$\begin{cases} F_{BX} = F_{1X}\cos\theta_{10} + F_{1Y}\sin\theta_{10} \\ F_{BY} = -F_{1X}\sin\theta_{10} + F_{1Y}\cos\theta_{10} \end{cases}. \tag{9}$$

3.3 Hydrodynamic model of tail fin

Based on the drag equation of flat plate[8], take the normal velocity of the barycenter of tail fin as the velocity of fluid, the hydrodynamic force of tail fin is given by the relation:

$$F_3 = C_3 \rho V_{C_3}^2 A_3 / 2, \tag{10}$$

where C_3 is the drag coefficient, V_{C_3} is the velocity component of the barycenter of tail fin on O_3Y_3, A_3 is the projected area of tail fin on the plane $X_3O_3Z_3$.

4 Dynamic simulation of robot fish

4.1 Virtual prototype of robot fish

The dynamic simulation of two-joint robot fish was conducted with the ADAMS software. Fig. 4 shows the dimensional parameters of robot fish virtual prototype (unit: mm). The front part of fish body is a half ellipsoid. The middle part of fish body is a cylinder. The end of fish body is a cone. There is a slot used to set the tail in the end of fish body. The tail of robot fish is a cane bar. The tail fin of robot fish is a thin rectangular plate.

During the dynamic simulation, the pitching motions of tail and tail fin are given by Eqs. (11) and (12).

$$\theta_{21} = \theta_{21\max} \sin(2\pi f t), \tag{11}$$

$$\theta_{31} = \theta_{31\max} \sin(2\pi f t - 90^\circ), \tag{12}$$

where f is the frequency of pitching motion, θ_{21} is the angle between O_2X_2 and O_1X_1, $\theta_{21\max}$ is the amplitude of θ_{21}, θ_{31} is the angle between O_3X_3 and O_1X_1, $\theta_{31\max}$ is the amplitude of θ_{31}. In this condition, the tail fin gains propulsive force in the whole pitching motion cycle.

Based on the hydrodynamic analysis, the hydrodynamic forces added on the robot fish are gained as follows.

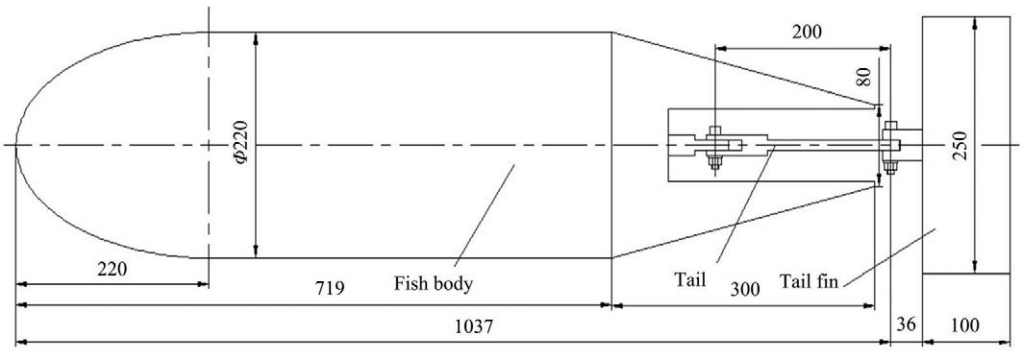

Fig. 4 Dimensional parameters of the robot fish virtual prototype.

(1) Hydrodynamic force of the tail fin. *Re* of *Thunniform* fish during swimming is much greater than 10^3, and the aspect ratio of tail fin is 2.5, thus[8]: $C_3 = 1.105$. Set the parameters as: $\rho = 1\times10^3$ kg·m^{-3} and $A_3 = 0.025$ m^2, then the hydrodynamic force of tail fin is gained by Eq. (10):

$$F_3 = C_3\rho V_{C_3}^2 A_3/2 = 1.105\times10^3\times V_{C_3}^2\times0.025/2 = 13.8125V_{C_3}^2. \quad (13)$$

(2) Hydrodynamic force of the fish body. Set the parameters as: A_X = 0.038 m^2, A_Y = 0.176 m^2, $L_0 = 1.019$ m and $L_1 = 0.574$ m. The profile of robot fish virtual prototype is similar to a torpedo. People have gained mass data about the drag coefficients of torpedo[8,9]. During the dynamic simulation, set drag coefficients as[8,9]: $C_{1X} = 0.4$, $C_{1Y} = 0.85$, and $C_{1S} = 0.85$, then the hydrodynamic forces of the fish body are gained by Eq.(8):

$$F_{BX} = \rho C_{1X}V_{XO_1}^2 A_X/2 = 10^3\times0.4\times V_{XO_1}^2\times0.038/2 = 7.6V_{XO_1}^2, \quad (14)$$

$$F_{BY} = \rho C_{1Y}V_{YO_1}^2 A_Y/2 = 10^3\times0.85\times V_{YO_1}^2\times0.176/2 = 74.8V_{YO_1}^2, \quad (15)$$

$$M_1 = \rho C_{1S}\dot{\theta}_{10}^2[(L_0-L_1)^4/L_1 + L_1^3]A_Y/8 = 10^3\times0.85\times\dot{\theta}_{10}^2\times[(1.019-0.574)^4/0.574 + 0.574^3]\times0.176/8 = 4.81\dot{\theta}_{10}^2. \quad (16)$$

4.2 Analysis of the swing of fish body

Fig. 3 shows the hydrodynamic forces of robot fish, and those hydrodynamic forces have been developed in subsection 4.1. Eqs. (13) to (16) are used to calculate forces on the robot fish in the dynamic simulation. The quantitative analysis of swing of fish body can be developed by ADAMS software, although errors between the simulation results and the true values are unavoidable.

In the dynamic simulation, m_1 indicates the mass of fish body, m_2 indicates the mass of tail and m_3 indicates the mass of tail fin. Set the parameters as: $m_2 = 0.3$ kg, $m_3 = 0.2$ kg and $\theta_{21\max} = \theta_{31\max} = 25^\circ$. The analysis mainly focuses on the following three problems:

(1) The relationship between the swing of fish body and the mass distribution of robot fish. During the simulation, set the pitching frequency of the tail as: $f = 2$ Hz, change m_1 by the density, Fig.5 shows the simulation results.

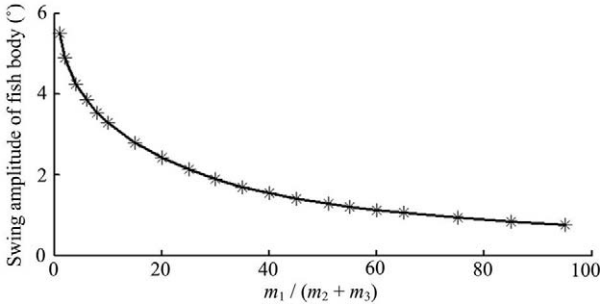

Fig. 5 Plot of the swing amplitude of fish body versus $m_1/(m_2+m_3)$.

The curve in Fig. 5 states that the swing amplitude of fish body reduces as $m_1/(m_2+m_3)$ increases, and the reduction of swing amplitude tends to be little when $m_1/(m_2+m_3)$ is larger than 50. Therefore, during the

design of robot fish, the swing of fish body could be restrained by increasing the mass of fish body and decreasing the masses of tail and tail fin.

(2) The relationship between swing of the fish body and pitching frequency of the tail. Set the mass of fish body as: $m_1 = 25.5$ kg, Fig. 6 and Fig. 7 show the simulation results by changing the pitching frequency of tail.

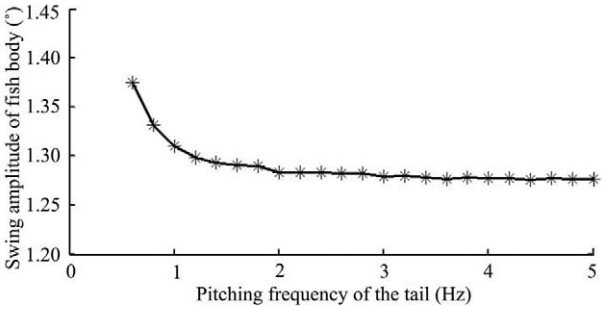

Fig. 6 Plot of the swing amplitude of fish body versus the pitching frequency of tail.

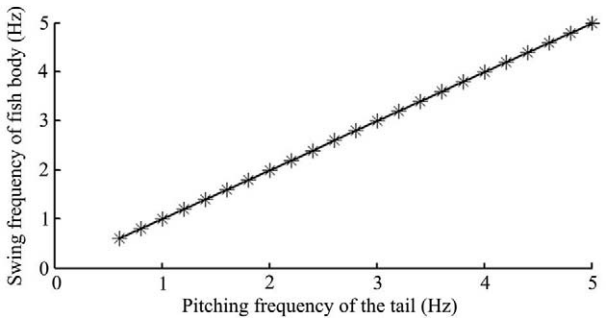

Fig. 7 Plot of the swing frequency of fish body versus the pitching frequency of tail.

The curve in Fig. 6 states that the swing amplitude of fish body decreases as the pitching frequency of tail increases from 0.6 Hz to 5 Hz, and when the pitching frequency of tail is larger than 2 Hz, the decrease in swing amplitude becomes minute. The curve in Fig. 7 states that the swing frequency of fish body is the same as the pitching frequency of tail.

(3) The impact of the swing of fish body on the motion parameters of tail fin. Set the pitching frequency of tail as: $f = 2$ Hz, and change m_1 to do the simulation. Fig. 8 shows the results. Curve 1 in Fig. 8 shows the relationship between the decrement of the heaving amplitude of tail fin and $m_1/(m_2 + m_3)$. Curve 2 in Fig. 8 shows the relationship between the decrement of the maximal attack angle of tail fin and $m_1/(m_2 + m_3)$.

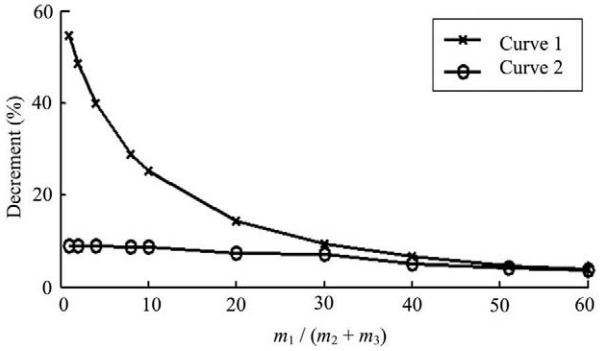

Fig. 8 Plot of the decrement of the maximal attack angle and heaving amplitude of tail fin versus $m_1/(m_2+m_3)$.

Curves in Fig. 8 state that the swing of fish body could reduce the heaving amplitude and the maximal attack angle of tail fin. The decrement of heaving amplitude increases with the decrease in $m_1/(m_2 + m_3)$, and it becomes distinct after $m_1/(m_2 + m_3)$ is smaller than 10. The decrement of maximal attack angle increases with the decrease in $m_1/(m_2 + m_3)$.

4.3 Restraint of the swing of fish body

The simulation results show that the swing of fish body reduces the heaving amplitude and changes the attack angle, which could impact the propulsive force and efficiency. Furthermore, the swing of fish body destroys the propulsive stability of robot fish and the reliable operating of sensor-based system. It is significant to study the methods to restrain the swing of fish body, and three ways are presented:

(1) Installation of dorsal fin and ventral fin. This idea is inspired by the real fish. The dorsal fin and ventral fin can increase $\boldsymbol{M}_1$ in Fig. 3, which inhibits the swing of fish body. The inhibition turns better as the effective areas of fins increase. But the dorsal fin and ventral fin may destroy the mobility of robot fish and increase the difficulty of sealing.

(2) Installation of vibration absorber. As shown in Fig. 9, a vibration absorber is set inside the fish body to restrain the swing. The vibration absorber contains an elastic element, a damping element and a mass element. k is the elastic coefficient, m is the mass, c is the damp coefficient. Set the parameters as: $f = 2$ Hz, $m_1 = 10$ kg, $k = 0$, $m = 1.0$ kg, change c during the simulation, Fig. 10 shows the simulation results.

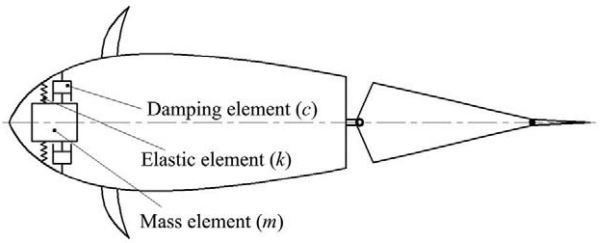

Fig. 9 Vibration absorber to restrain the swing of fish body.

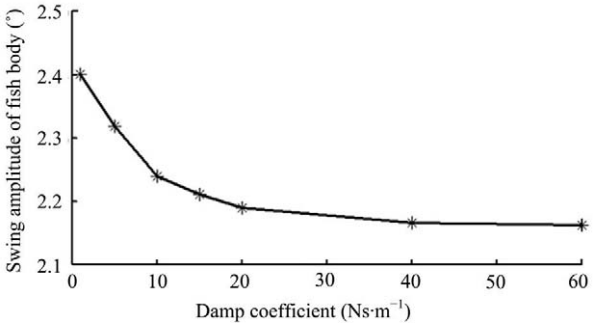

Fig. 10 Plot of the swing amplitude of fish body versus the damp coefficient of vibration absorber.

Fig. 10 states that the swing amplitude of fish body decreases as c increases, and the decrease become minute when c is larger than 40 N·s·m^{-1}. Therefore, a vibration absorber with rational parameters could restrain the swing of fish body. This method has no effect on the surface of robot fish, which makes the sealing very simple.

(3) Robot fish with parallel tails. The swing of fish body is caused by the cross components of the hydrodynamic force and apparent force of tail and tail fin. So methods making the cross components of hydrodynamic force and apparent force equal to zero could ensure the robot fish swimming with no swing of fish body. Then the idea that the robot fish with parallel tails was presented. The same two tails work with symmetrical pitching motion, and the cross components of hydrodynamic force and apparent force cancel out reciprocally, which eliminats the swing motion of fish body finally. Then the robot fish could work with the given motion parameters of tail fin. Furthermore, the robot fish with parallel tails could do smart turning with one tail works and the other one keeps rest.

A parallel robot fish virtual prototype was developed to test the specialty of robot fish with parallel tail. The parallel robot fish virtual prototype contains two robot fish in Fig. 4 and connects two fish bodies together. One tail pitches as Eqs. (11) and (12), and the other tail pitches with symmetrical motion. Then the tails gain propulsive force in the whole pitching motion cycle. The hydrodynamic forces were added on each single robot fish respectively according to Eqs. (13) to (16). Set parameters as: $m_1 = 25.5$ kg, $m_2 = 0.3$ kg, $m_3 = 0.2$ kg and $\theta_{21\max} = \theta_{31\max} = 25^\circ$, change the pitching frequency of tail to do dynamic simulation, Fig. 11 shows the results.

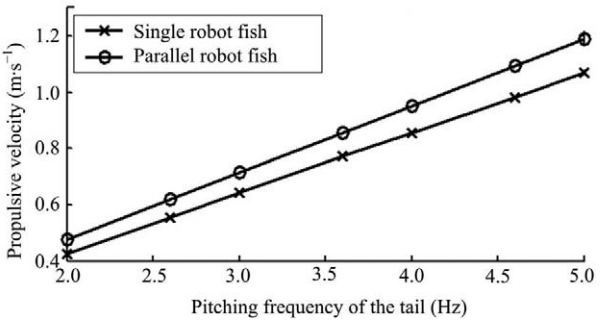

Fig. 11 Plot of the swimming velocity of robot fish versus the swing frequency of tail.

Fig. 11 states that parallel robot fish gains higher propulsive velocity compared with the single robot fish. Dynamic simulation of the robot fish with parallel tails shows that the parallel robot fish has no swing motion of fish body.

5 Conclusion

The disadvantages of the swing of fish body were analyzed. The hydrodynamic analysis of two-joint robot fish was developed, and the models of the hydrodynamic force of fish body and tail fin were built. The dynamic simulation of robot fish was finished with the ADAMS software. The simulation results show:

(1) The swing amplitude of fish body reduces as $m_1/(m_2+m_3)$ increases, and the decrease of swing amplitude tends to be little after $m_1/(m_2+m_3)$ is larger than 50. During the design of robot fish, the swing of fish body could be restrained by increasing the masses of fish body and decreasing the masses of tail and tail fin.

(2) The swing amplitude of fish body decreases as the pitching frequency of tail increases.

(3) The swing frequency of fish body is as same as the pitching frequency of tail.

(4) The swing of fish body could reduce the heaving amplitude and maximal attack angle of tail fin. The decrement of heaving amplitude increases with the decrease in $m_1/(m_2+m_3)$, and becomes distinct after $m_1/(m_2+m_3)$ is smaller than 10.

Based on the simulation results, three methods to restrain the swing of fish body are presented:

(1) Installation of dorsal fin and ventral fin. The structure of robot fish would be very simple, but the dorsal fin and ventral fin may destroy the mobility of the robot fish, and make the sealing difficulty.

(2) Installation of vibration absorber. This method makes the sealing very simple.

(3) Robot fish with parallel tails. This method eliminates the swing motion of fish body. Furthermore, the robot fish with parallel tails could do smart turning with one tail works and the other one keeps rest.

During the simulation, the hydrodynamic force of tail was ignored, which could result in the errors between the simulation results and the true values. But considering that the hydrodynamic force of tail is minute, the simulation results could describe the motion of robot fish. The simulation results could guide the design of robot fish.

Acknowledgement

This work was supported by the National Natural Science Foundation (Grant No. 59705011).

References

[1] Wu T Y. Swimming of waving plate. *Journal of Fluids Mechanics*, 1961, **10**, 321–344.

[2] Lightill M J. Aquatic animal propulsion of high hydromechanical efficiency. *Journal of Fluids Mechanics*, 1970, **44**, 265–301.

[3] Lightill M J. Large amplitude elongated-body theory of fish locomotion. *Proceedings of Royal Society of London*, 1971, **179**, 125–138.

[4] Chopra M G, Kambe T. Hydromechanics of lunate-tail swimming propulsion. Part 2. *Journal of Fluid Mechanics*, 1977, **79**, 49–69.

[5] Tong B G, Zhuang L X, Cheng J Y. Hydrodynamics research on wavelike pitching motion propulsion of fish. *Mechanics and Engineering*, 1991, **13**, 17–26. (in Chinese)

[6] Su Y M, Huang S, Pang Y J, Xu Y R, Wu Q. Hydrodynamic analysis of submersible propulsion system imitating tuna-tail. *The Ocean Engineering*, 2002, **20**, 54–59. (in Chinese)

[7] Sfakiotakis M, Lane D M, Davies J B C. Review of fish swimming modes for aquatic locomotion. *IEEE Journal of Oceanic Engineering*, 1999, **24**, 237–252.

[8] Xia T C. *Engineering Fluid Mechanics*, Shanghai Jiao Tong University Press, Shanghai, 2006. (in Chinese)

[9] He M L. *Studying on Hydrodynamic Characteristics of AUV with Numerical Model and Experiments*, Dissertation for Doctor Degree of Tianjin University, Tianjin, 2005. (in Chinese)